



Selenate removal in biofilm systems: effect of nitrate and sulfate on selenium removal efficiency, biofilm structure and microbial community

Authors: Lea Chua Tan, Erika J. Espinosa - Ortiz, Yarlagadda V. Nancharaiah, Eric D. van Hullebusch, Robin Gerlach, and Piet N. L. Lens

This is the peer reviewed version of the following article: see citation below, which has been published in final form at <https://doi.org/10.1002/jctb.5586>. This article may be used for non-commercial purposes in accordance with Wiley Terms and Conditions for Self-Archiving.

Tan, Lea Chua, Erika J. Espinosa - Ortiz, Yarlagadda V. Nancharaiah, Eric D. van Hullebusch, Robin Gerlach, and Piet N. L. Lens, "Selenate removal in biofilm systems: effect of nitrate and sulfate on selenium removal efficiency, biofilm structure and microbial community," Journal of Chemical Technology & Biotechnology, January 2018. doi:10.1002/jctb.5586

Selenate removal in biofilm systems: effect of nitrate and sulfate on selenium removal efficiency, biofilm structure and microbial community

Lea Chua Tan,^{a*} Erika J Espinosa-Ortiz,^b Yarlagadda V Nancharaiah,^c Eric D van Hullebusch,^{a,d} Robin Gerlach^b and Piet NL Lens^{a,e}

Abstract

BACKGROUND: Selenium (Se) discharged into natural waterbodies can accumulate over time and have negative impacts on the environment. Se-laden wastewater streams can be treated using biological processes. However, the presence of other electron acceptors in wastewater, such as nitrate (NO_3^-) and sulfate (SO_4^{2-}), can influence selenate (SeO_4^{2-}) reduction and impact the efficiency of biological treatment systems.

RESULTS: SeO_4^{2-} removal by biofilms formed from an anaerobic sludge inoculum was investigated in the presence of NO_3^- and SO_4^{2-} using drip flow reactors operated continuously for 10 days at pH 7.0 and 30 °C. The highest total Se (~60%) and SeO_4^{2-} (~80%) removal efficiencies were observed when the artificial wastewater contained SO_4^{2-} . A maximum amount of 68 $\mu\text{mol Se cm}^{-2}$ was recovered from the biofilm matrix in $\text{SO}_4^{2-} + \text{SeO}_4^{2-}$ exposed biofilms and biofilm mass was 2.7-fold increased for biofilms grown in the presence of SO_4^{2-} . When SeO_4^{2-} was the only electron acceptor, biofilms were thin and compact. In the simultaneous presence of NO_3^- or SO_4^{2-} , biofilms were thicker (> 0.6 mm), less compact and exhibited gas pockets.

CONCLUSION: The presence of SO_4^{2-} had a beneficial effect on biofilm growth and the SeO_4^{2-} removal efficiency, while the presence of NO_3^- did not have a significant effect on SeO_4^{2-} removal by the biofilms.

© 2018 Society of Chemical Industry

Supporting information may be found in the online version of this article.

Keywords: biofilm; co-electron acceptors; selenium removal; biofilm characterization; selenate; nitrate; sulfate

INTRODUCTION

Selenium (Se) is a trace metalloid that is vital, but at the same time harmful, to living organisms, with an unusually small concentration range of only 5- to 10-fold difference between essential and toxic concentrations.¹ Apart from naturally occurring processes that mobilize Se from minerals and volcanic rocks, anthropogenic activities (i.e. mining and agriculture) are the major contributors of Se mobilization and release into the environment.² Se oxyanions such as selenite (SeO_3^{2-}) and selenate (SeO_4^{2-}) are typically found at low levels (< 12 mg Se L⁻¹) in drainage, acid rock drainage and mining wastewaters compared with other contaminants like nitrate (NO_3^-) and sulfate (SO_4^{2-}) which are typically present at 250 mg L⁻¹ and 3000 mg L⁻¹, respectively.³ Se is considered a problematic pollutant because it has the propensity to bioaccumulate in organisms.⁴ Se release and accumulation into the aquatic environment has posed serious threats to egg-laying vertebrates, causing reproductive failures and teratogenic effects, which subsequently resulted in monetary losses of millions of dollars to fisheries.⁵ Due to the environmental impacts of Se release into the aquatic environment, Se removal from contaminated waters

before discharge is essential for the protection of living organisms and the environment.

Membrane filtration, ion exchange, adsorption and chemical reduction methods are typically used for Se removal from contaminated waters.³ However, the use of biological methods is

* Correspondence to: LC Tan, UNESCO-IHE Institute for Water Education, Westvest 7, 2611 AX Delft, The Netherlands. E-mail: lea_chua_tan@yahoo.com

a UNESCO-IHE Institute for Water Education, Delft, The Netherlands

b Department of Chemical and Biological Engineering, Center for Biofilm Engineering, Montana State University, Bozeman, USA

c Water and Steam Chemistry Division, Bhabha Atomic Research Centre, Tamil Nadu, India

d Université Paris-Est, Laboratoire Géomatériaux et Environnement, Marne-la-Vallée, France

e Department of Chemistry and Bioengineering, Tampere University of Technology, Tampere, Finland

becoming attractive because these methods offer an environmentally friendly and potentially cost-effective alternative, might be suitable for large-scale application and might allow for biogenic elemental Se (Se^0) recovery.⁶ The biological process converts the soluble Se oxyanions to insoluble and less toxic Se^0 ,⁷ which can potentially be recovered and reused for various industrial applications, such as fertilizers for Se-deficient soils or use in photovoltaic cells.^{8,9} Despite the recent advances in the biological treatment of Se-laden wastewaters, there are still many knowledge gaps in the application of the treatment, particularly when considering the complexity of Se-laden wastewaters. One of the challenges of Se-laden wastewaters, such as mining effluents, is the presence of other oxyanions, such as NO_3^- and SO_4^{2-} , that are typically present in concentrations more than 100 to 1000 times greater than Se^3 .

NO_3^- and SO_4^{2-} are terminal electron acceptors for denitrifying and sulfate-reducing bacteria, respectively, and can either inhibit or enhance microbial SeO_4^{2-} removal by microorganisms.³ Orem-lund *et al.*¹⁰ observed that the presence of NO_3^- (0.1 mmol L⁻¹) promoted the ability of *Sulfospirillum barnesii* to reduce SeO_4^{2-} (0.1 mmol L⁻¹) by keeping the cells in a constant state of high metabolic activity. In contrast, Lai *et al.*¹¹ reported a 30% decrease in SeO_4^{2-} (0.02 mmol L⁻¹) removal in a hydrogen-based membrane biofilm reactor (MBfR) in the presence of NO_3^- (<0.9 mmol L⁻¹), attributed to competition for H_2 (electron donor) and possible suppression of the SeO_4^{2-} reductases. A study by Hockin and Gadd¹² using a sulfate-reducing biofilm composed of *Desulfomicrobium norvegicum* carried out SeO_4^{2-} removal and suggested greater SeO_4^{2-} reduction in the presence of excess SO_4^{2-} (28 mmol L⁻¹) compared with SO_4^{2-} limiting conditions (5 mmol L⁻¹). In contrast, Ontiveros-Valencia *et al.*¹³ did not observe any change in the removal efficiency of SeO_4^{2-} (< 0.08 mmol L⁻¹) by an anaerobic biofilm growing in a hydrogen-fed membrane reactor in the presence or absence of SO_4^{2-} .

Most studies have focused on SeO_4^{2-} reduction in the presence of either NO_3^- or SO_4^{2-} , while only a few studies have conducted an in-depth analysis of the effect of the concurrent presence of NO_3^- and SO_4^{2-} on SeO_4^{2-} reduction in biological systems. In a previous study using anaerobic granular sludge,¹⁴ there was an observable impact of NO_3^- and SO_4^{2-} on SeO_4^{2-} removal efficiencies. In addition, the effect Se might have on biomass growth, Se speciation and Se^0 fate in the presence of NO_3^- and/or SO_4^{2-} have yet to be reported, particularly in a biofilm system. There are only limited studies on SeO_4^{2-} removal and biofilm–Se interactions with co-electron acceptors, most of which were investigated using MBfRs with H_2 as electron donor.^{13,15} Therefore, this study investigates the responses of lactate-fed anaerobic biofilms growing in drip flow reactors (DFRs) to SeO_4^{2-} and other electron acceptors (SO_4^{2-} and NO_3^-) by determining: (i) the impact on the SeO_4^{2-} removal efficiency; and (ii) changes in biofilm characteristics, including biofilm architecture and microbial community composition.

MATERIALS AND METHODS

Inoculum and biofilm growth conditions

Anaerobic granular sludge taken from a full-scale upflow anaerobic sludge bed (UASB) reactor treating paper-mill wastewater (Eerbeek, The Netherlands) was used as the inoculum¹⁶ for biofilm development. About 1 g of wet granular sludge was homogenized using a homogenizer potter tube and used as the seed inoculum (0.25 g dry weight). All experiments were carried out using

synthetic mining wastewater composed of growth medium, electron donor and the three oxyanions under study.

The composition of the growth medium, according to Tan *et al.*,¹⁴ was as follows (in g L⁻¹): NH_4Cl (0.30), $\text{CaCl}_2 \cdot 2\text{H}_2\text{O}$ (0.10), $\text{MgCl}_2 \cdot 6\text{H}_2\text{O}$ (0.01) and NaHCO_3 (0.04). Phosphate buffer (0.053 g L⁻¹ Na_2HPO_4 and 0.041 g L⁻¹ KH_2PO_4) was included in the medium to maintain near neutral pH (7–8) conditions. Acid and alkaline trace metal solutions (0.1 mL each, as described in Stams *et al.*¹⁷) were added to 1 L of synthetic wastewater. Sodium lactate was used as the electron donor while NO_3^- , SO_4^{2-} and SeO_4^{2-} (provided as KNO_3 , K_2SO_4 and Na_2SeO_4) were provided as electron acceptors. Assuming complete oxidation of lactate and reduction of oxyanions to Se^0 , N_2 and HS^- , 1 mole of SeO_4^{2-} , NO_3^- and SO_4^{2-} requires 0.4, 0.6 and 0.8 moles of COD, respectively. All feed solutions were purged with nitrogen gas to remove oxygen from the artificial wastewater. It should be noted that the synthetic mine wastewater used in this study simulates, as closely as possible, the composition of Se-laden wastewater in the mining industry as described in Stover *et al.*¹⁸

Reactor configuration

Drip flow reactors (DFRs) provide plug flow-like systems under low-shear/laminar flow and are flexible and adaptable to a variety of conditions.¹⁹ Multi-panel DFRs (15.24 cm × 12.70 cm × 2.54 cm) (Supplementary material, Figure S1) were used with silicon coupons (0.3 cm × 7.5 cm × 2.5 cm) as the substratum for biofilm growth. Each DFR was assembled according to Goeres *et al.*¹⁹ Biofilms were cultivated under anoxic conditions at 30 °C for a total period of 12 days. All DFR incubations were performed at least in duplicate. Effluent liquid samples were collected daily and analyzed for lactate, NO_3^- , SO_4^{2-} and Se concentrations (total Se, SeO_4^{2-} and SeO_3^{2-}).

DFRs were initially purged with N_2 while all influent solutions were purged with N_2 for 30 min and changed every 2 days. Each DFR was initially inoculated with 1 g homogenized wet granules in 10 mL with only lactate and growth medium (without oxyanions). Each DFR was operated in batch mode for 2 days to allow for the attachment and growth of cells on the substratum. After 2 days, the DFR was inclined at a 10° angle and operated continuously at a flow rate of 0.2 mL min⁻¹ (0.288 L day⁻¹) for 10 days. During the continuous operation, biofilms were exposed to 20 mmol L⁻¹ lactate and the following conditions: (a) no electron acceptors, (b) $\text{NO}_3^- + \text{SO}_4^{2-}$, (c) SeO_4^{2-} , (d) $\text{NO}_3^- + \text{SeO}_4^{2-}$, (e) $\text{SO}_4^{2-} + \text{SeO}_4^{2-}$ and (f) $\text{NO}_3^- + \text{SO}_4^{2-} + \text{SeO}_4^{2-}$. SeO_4^{2-} , NO_3^- and SO_4^{2-} were provided at average concentrations of 0.13 (± 0.02) mmol L⁻¹, 4.8 (± 0.3) mmol L⁻¹ and 12.9 (± 0.3) mmol L⁻¹, respectively.

Biofilm characterization

Biofilms grown under different conditions on the silicon coupons were cut into sections for various analyses at the end of each experimental run. Biofilm samples were scraped from the silicon coupon into a micro-centrifuge tube (pre-weighed) for measurement of wet biomass weight. The biofilm dry weight, ash-free dry weight and total Se in the biofilm per area (cm²) was determined. Dry weight was reported as total solids (TS), while ash-free dry weight was reported as volatile solids (VS).

Biofilm dry weight and ash-free dry weight were measured following standard protocols. Biomass was first dried in an incubator at 100 °C for 3 days (dry weight) followed by heating in a furnace at 500 °C for 4 h (ash-free weight). Biofilm samples (two samples per coupon) for total Se content were first digested using concentrated nitric acid (HNO_3) for 2 days, centrifuged and diluted using

5% HNO₃ (modified from Jain *et al.*²⁰). Total Se was then analyzed using inductively coupled plasma mass spectrometry (ICP-MS, Agilent 7500ce). Cell viability was analyzed using the Live/Dead[®] BacLight™ Bacterial Viability kit containing SYTO9 and propidium iodide (PI);²¹ green ('live') and red ('dead') cells were counted using epifluorescence microscopy (Nikon Eclipse E800).

Biofilm imaging

The architecture of the biofilms formed under different operating conditions was visualized using a Leica TCS-SP2 AOBs confocal laser scanning microscope (CLSM). Biofilms formed on the silicon coupons were first stained using the Live/Dead[®] BacLight™ kit for 20 min at 30 °C in the dark. Excess dye was removed by washing with pure water and images were taken at 100× and 630× magnifications. Imaris software (Bitplane Scientific Software) was used for processing the CLSM images.

Biofilm thickness was estimated using a cryo-section method. Briefly, stained biofilm samples were frozen by placing them on dry ice and covering with a tissue embedding medium (OCT, optimum cutting temperature, Tissue-Tek). Samples were sliced into 5 μm sections using a Leica CM1850 cryostat at -20 °C. Images were acquired using a Nikon Eclipse E800 microscope in fluorescence and transmission modes using differential interference contrast optics and processed for thickness measurements using MetaMorph (Molecular Devices). Five samples were analyzed per reactor for thickness measurements.

The elemental composition of the biofilm matrix was analyzed using a scanning electron microscope (SEM, Zeiss Supra™ 55VP) equipped with an energy dispersive X-ray spectroscopy unit (EDX, Princeton Gamma-Tech) using secondary electron and back-scattering mode. For SEM analysis, the biofilm samples were gently washed with Milli-Q water and dried at ambient temperature and pressure. Dried samples were deposited onto carbon tape and coated with iridium before imaging.

Microbial community analysis

Genomic DNA was extracted from the samples following the protocol of Lueders *et al.*²² and quantified using a NanoDrop-1000 spectrophotometer. Extracted DNA was amplified by PCR using primers Pro 341 forward and Pro 805 reverse targeting the V4 region of the 16S rRNA gene of bacteria and archaea.²³ Amplicons were checked by agarose gel electrophoresis and sequenced using the Illumina MiSeq standard protocol sequencing platform '16S Metagenomic Sequencing Library Preparation'. Sequences produced were analyzed using the standard operating procedures of the bioinformatics platform Mothur.²⁴

Analytical methods

Effluent samples were collected daily and filtered using 0.2 μm cellulose acetate membranes. Filtered samples were analyzed for lactate, NO₃⁻, SO₄²⁻ and SeO₄²⁻ using ion chromatography (IC, Dionex ICS-1100). The IC column used was a Dionex Ion Pac™ AS22, operation was set at 1.2 mL min⁻¹ flow rate, using a 25 μL sample loop with 4.5 mmol L⁻¹ Na₂CO₃ and 1.4 mmol L⁻¹ NaHCO₃ as eluent. The SeO₃²⁻ concentrations were determined using a spectrophotometric method.²⁵ Briefly, 1 mL of sample was mixed with 0.5 mL of 4 mol L⁻¹ HCl and 1 mL of 1 mol L⁻¹ ascorbic acid; after 10 min, absorbance was measured at 500 nm using a Genesys 10UV scanning spectrophotometer (Thermo Scientific) and compared with the absorbance of equivalently treated standards with known SeO₃²⁻ concentrations. Total dissolved sulfides were determined

colorimetrically as well (at 480 nm) after the formation of a colloidal copper sulfide precipitate as described by Cord-Ruwisch.²⁶ Unfiltered liquid samples were acidified with HNO₃ and measured for total Se using ICP-MS. At the end of each experiment, effluent samples (50 mL) were collected and dried at room temperature. Dried particles were analyzed for elemental components using SEM-EDX as described above.

Reactor performance parameters and statistical analysis

Average daily removal rates and removal efficiencies for lactate, NO₃⁻, SO₄²⁻, SeO₄²⁻ and total Se were calculated. The removal rates were calculated according to Equation (1):

$$\text{Removal rate (mmol per day)} = Q \times (C_{in} - C_{out}) \quad (1)$$

where Q is flow rate in L day⁻¹ while C_{in} and C_{out} are, respectively, influent and effluent concentration in mmol L⁻¹. Statistical differences were evaluated using analysis of variance (ANOVA) with Tukey test method for multiple comparison; a $P_{\text{value}} \leq 0.05$ was considered statistically significantly different.

RESULTS

Effect of co-electron acceptors on Se removal

The pH values in the DFRs remained close to neutral for all experimental runs with the measured effluent pH ranging from 7.0–8.0 for all DFR incubations. Table 1 shows the removal performance of the DFRs under different incubation conditions. Total Se and SeO₄²⁻ removal rates were highest for the treatments receiving SO₄²⁻ (SO₄²⁻ + SeO₄²⁻ and SO₄²⁻ + NO₃⁻ + SeO₄²⁻), attaining an average of 61 (±2)% total Se and 77 (±1)% SeO₄²⁻ removal efficiency. The highest SeO₃²⁻ concentration detected in the effluent amounted to 0.04 (±0.01) mmol L⁻¹ for biofilms exposed to both SeO₄²⁻ and SO₄²⁻, while the other incubations had an average SeO₃²⁻ concentration of 0.02 (±0.01) mmol L⁻¹. Significantly lower SeO₄²⁻ removal ($P_{\text{value}} \leq 0.0001$) was observed by the DFR biofilms grown in the absence of SO₄²⁻ (SeO₄²⁻ and NO₃⁻ + SeO₄²⁻). DFR incubations with SeO₄²⁻ alone attained 17 (±9)% total Se and 30 (±6)% SeO₄²⁻ removal efficiencies, while NO₃⁻ + SeO₄²⁻ incubations attained 17 (±2)% total Se and 37 (±12)% SeO₄²⁻ removal efficiencies.

NO₃⁻ removal in the DFR biofilm systems was successfully achieved (~97%) when grown with SO₄²⁻ (Table 1). Low NO₃⁻ removal (56 ± 17%) was observed in the absence of SO₄²⁻ (Table 1). SO₄²⁻ removal was low for all experimental conditions, reaching only a 7 mmol day⁻¹ removal rate compared with the influent SO₄²⁻ mass flow rate of 44 mmol day⁻¹. However, there was a significant increase ($P_{\text{value}} = 0.009$) in the SO₄²⁻ removal efficiency from 5% to 15% in the absence of SeO₄²⁻.

Biofilm characterization under different growth conditions

Biofilm structure

Images of biofilms grown under different incubation conditions are shown in Fig. 1. In the absence of oxyanions, biofilms on the silicone coupons were whitish and fairly transparent. Biofilms exposed to SeO₄²⁻ or NO₃⁻ + SeO₄²⁻ developed a light orange coloration, while biofilms exposed to SO₄²⁻ + SeO₄²⁻ (with or without the presence of NO₃⁻) showed intense red coloration with interspersed whitish to yellowish deposits. CLSM images did not reveal significant morphological or architectural differences among the biofilms grown under the different conditions (Fig. S2).

Table 1. Average removal performance (daily removal rate and removal efficiency) in the drip flow reactor for lactate, NO_3^- , SO_4^{2-} and Se (total Se and SeO_4^{2-}). Lactate, NO_3^- , SO_4^{2-} and SeO_4^{2-} were provided at the following rates in mmol day^{-1} : 61 (± 6), 16 (± 2), 44 (± 3) and 0.50 (± 0.03), respectively

| Incubation units | | A* | B** | C* | D** | E** | F* |
|----------------------------|------------------------|-------------------|------------------------------------|---------------------|-------------------------------------|--|--|
| | | No electron donor | $\text{NO}_3^- + \text{SO}_4^{2-}$ | SeO_4^{2-} | $\text{NO}_3^- + \text{SeO}_4^{2-}$ | $\text{SO}_4^{2-} + \text{SeO}_4^{2-}$ | $\text{NO}_3^- + \text{SO}_4^{2-} + \text{SeO}_4^{2-}$ |
| Daily removal rate: | | | | | | | |
| Lactate | mmol day^{-1} | 38 (± 19) | 58 (± 5) | 32 (± 15) | 29 (± 3) | 57 (± 3) | 42 (± 12) |
| NO_3^- | mmol day^{-1} | - | 18 (± 1) | - | 9 (± 2) | - | 13 (± 1) |
| SO_4^{2-} | mmol day^{-1} | - | 7 (± 5) | - | - | 4 (± 2) | 4 (± 1) |
| Total Se | mmol day^{-1} | - | - | 0.07 (± 0.04) | 0.08 (± 0.06) | 0.30 (± 0.05) | 0.30 (± 0.08) |
| SeO_4^{2-} | mmol day^{-1} | - | - | 0.10 (± 0.03) | 0.20 (± 0.07) | 0.40 (± 0.09) | 0.40 (± 0.07) |
| Removal efficiency: | | | | | | | |
| Lactate | % consumed | 62 (± 4) | 90 (± 12) | 54 (± 9) | 42 (± 14) | 89 (± 12) | 79 (± 10) |
| NO_3^- | % removed | - | 99 (± 1) | - | 56 (± 17) | - | 95 (± 9) |
| SO_4^{2-} | % removed | - | 15 (± 11) | - | - | 5 (± 3) | 5 (± 2) |
| Total Se | % removed | - | - | 17 (± 9) | 17 (± 2) | 59 (± 11) | 62 (± 18) |
| SeO_4^{2-} | % removed | - | - | 30 (± 6) | 37 (± 12) | 77 (± 15) | 76 (± 13) |

*n = 4 experimental replicates;
**n = 2 experimental replicates.

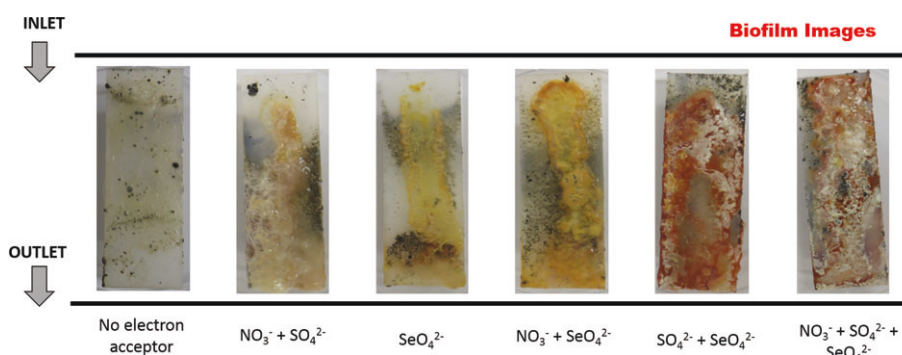


Figure 1. Representative images of biofilms formed under the different incubation conditions. Images were taken using a digital camera; silicon coupons were 2.5 cm wide and 7.5 cm long.

Biofilm thicknesses were determined from cross-section images as shown in Fig. 2. In general, all biofilms had a thickness greater than 0.6 mm, except those grown with SeO_4^{2-} only. Empty spaces were observed in the biofilms, presumably voids or gas pockets within the biofilm matrix (indicated by red arrows in Fig. 2). Even though analyses of these gases was not performed in this study, these gas pockets in the biofilms are likely due to the microbial production of gases such as hydrogen sulfide, nitrogen gas, hydrogen or carbon dioxide. Gas bubbles were also visible along some of the biofilms (Fig. 1), particularly those biofilms grown in the presence of SO_4^{2-} . Biofilms exposed to SeO_4^{2-} showed a more compact structure (Fig. 2(c)), with a significantly lower average biofilm thickness of 0.20 (± 0.08) mm ($P_{\text{value}} \leq 0.0001$).

Biomass weight and biofilm activity

Dry weight of biofilms varied significantly among different incubations as shown in Table 2. Incubations exposed to SO_4^{2-} resulted in increased dry weights (6.6 ± 0.4 mg TS cm^{-2}) compared with incubations without SO_4^{2-} (2.5 ± 1.2 mg TS cm^{-2}). Ash-free dry weight results showed that the biofilms were mainly composed of organic materials (>70% were volatile matter) for all incubations (Table 2).

Biofilm activity was assessed through lactate consumption (Table 1) and cell viability (Fig. S3). Lactate was supplied as the sole external electron donor for all biofilm experiments and was

Table 2. Biomass dry weight and ash-free dry weight of biofilms from each incubation. Dry weight was reported as total solids (TS), while ash-free dry weight was reported as volatile solids (VS)

| Incubation | | Biofilm biomass | |
|------------|--|--------------------------------------|---|
| | | Dry weight (mg TS cm^{-2}) | Ash-free dry weight (mg VS cm^{-2}) |
| A* | No electron acceptor | 1.8 (± 0.7) | 1.4 (± 0.4) |
| B** | $\text{NO}_3^- + \text{SO}_4^{2-}$ | 6.6 (± 1.8) | 6.0 (± 1.4) |
| C* | SeO_4^{2-} | 1.9 (± 0.6) | 1.9 (± 0.9) |
| D** | $\text{NO}_3^- + \text{SeO}_4^{2-}$ | 3.9 (± 1.3) | 3.6 (± 1.2) |
| E** | $\text{SO}_4^{2-} + \text{SeO}_4^{2-}$ | 7.1 (± 1.2) | 6.4 (± 1.4) |
| F* | $\text{NO}_3^- + \text{SO}_4^{2-} + \text{SeO}_4^{2-}$ | 6.3 (± 1.1) | 4.0 (± 1.5) |

*n = 4 experimental replicates;
**n = 2 experimental replicates.

provided in excess at an average of 18.5 (± 0.9) mmol L^{-1} (at a rate of 61 mmol day^{-1}). Under conditions where no external electron acceptor was present, about 62 (± 4)% of the lactate was consumed. Incubations grown with SeO_4^{2-} alone and $\text{NO}_3^- + \text{SeO}_4^{2-}$ showed similar lactate consumption, averaging 54 (± 9)% and 42 (± 14)%, respectively. In contrast, biofilms grown in the presence

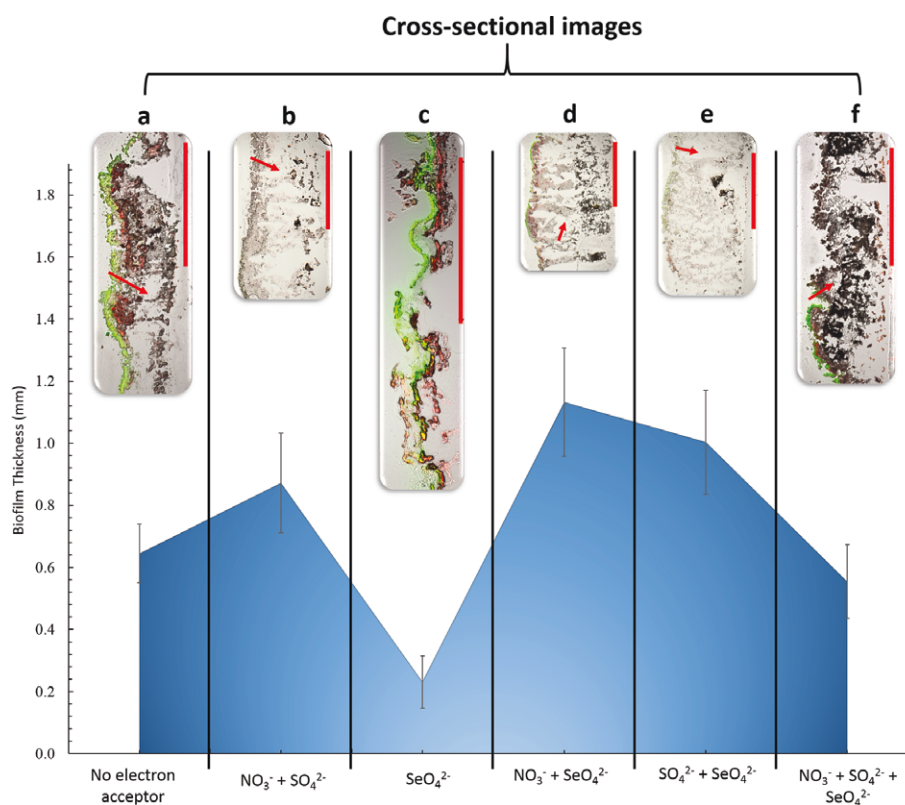


Figure 2. Cross-sectional images of biofilms stained with SYTO 9 (green) and propidium iodide (red) with corresponding thickness measurement in mm (area graph). All images were obtained using transmission and fluorescence microscopy under 40 \times magnification. Each scale bar (red line) represents 1 mm. Red arrows indicate presumed gas pockets observed in the cross-sectional images.

of SO_4^{2-} ($\text{NO}_3^- + \text{SO}_4^{2-}$ and $\text{SO}_4^{2-} + \text{SeO}_4^{2-}$) exhibited significantly higher lactate consumption rates of $52 (\pm 9) \text{ mmol day}^{-1}$, corresponding to a removal efficiency of $86 (\pm 6)\%$. Cell viability analysis showed that biofilms exposed to SeO_4^{2-} alone had the highest viable cell counts per unit area ($3.9 \times 10^8 \pm 1.3 \times 10^8$ viable cell counts/cm 2 , $P_{\text{value}} \leq 0.004$) compared with the other DFR incubations (Fig. S3). The $\text{SO}_4^{2-} + \text{SeO}_4^{2-}$ exhibited the lowest cell viability at $2.9 \times 10^7 (\pm 8.5 \times 10^6)$ viable cell counts cm $^{-2}$, which was 11 times lower than for the SeO_4^{2-} incubations.

Microbial community composition

Relative abundances (RA) at the bacterial family level were determined for each incubation (Fig. 3). Biofilms that developed in the absence of electron acceptors (fed with lactate alone) showed a similar relative abundance of *Firmicutes* ($38.3 \pm 9.8\%$ RA) and *Proteobacteria* ($43.1 \pm 10.0\%$ RA). On the other hand, biofilms grown with external electron acceptors were mainly composed of *Bacteroidetes*, *Firmicutes* and *Proteobacteria* ($98.8 \pm 0.5\%$ RA) of which *Proteobacteria* accounted for $65.2 (\pm 7.4)\%$ RA.

Biofilms incubated with SeO_4^{2-} alone developed *Pseudomonadaceae* ($19.8 \pm 5.3\%$ RA) as the dominant bacterial family of which 90% were associated with *Pseudomonas* spp. Common phylotypes of *Comamonadaceae* ($\sim 10.9\%$ RA), *Rhizobiaceae* ($\sim 18.5\%$ RA) and *Brucellaceae* ($\sim 12.9\%$ RA) were observed in the biofilms grown with SeO_4^{2-} alone and $\text{NO}_3^- + \text{SeO}_4^{2-}$ DFR incubations. Biofilms incubated in the presence of SO_4^{2-} developed similar communities dominated by *Campylobacteraceae*, *Rhodocyclaceae*, *Brucellaceae* and unclassified members of *Firmicutes* at an average of $15.5 (\pm 3.8)\%$, $14.3 (\pm 3.0)\%$, $12.3 (\pm 3.1)\%$ and $12.7 (\pm 1.1)\%$ RA, respectively.

Se concentration in the biofilm

Biofilms formed in the presence of $\text{SO}_4^{2-} + \text{SeO}_4^{2-}$ showed the highest amount of Se entrapped in the biofilm matrix at $68 (\pm 32) \mu\text{mol Se cm}^{-2}$, while $25 (\pm 18) \mu\text{mol Se cm}^{-2}$ was obtained for biofilms grown with $\text{NO}_3^- + \text{SO}_4^{2-} + \text{SeO}_4^{2-}$. Biofilms formed in conditions without SO_4^{2-} showed $< 5 \mu\text{mol Se cm}^{-2}$ entrapped in the biofilm matrix. An overall Se mass balance for the biofilm system was calculated (Table S1). For 10 days continuous operation, an average of $0.38 (\pm 0.03) \text{ mmol Se}$ ($30 \pm 2 \text{ mg Se}$) passed through the DFR. For SeO_4^{2-} and $\text{NO}_3^- + \text{SeO}_4^{2-}$ incubations, roughly 88 ($\pm 1\%$)% of Se was detected in the effluent while only 2 ($\pm 0.8\%$)% was entrapped in the biofilm (Table S1). In contrast, $\text{SO}_4^{2-} + \text{SeO}_4^{2-}$ and $\text{NO}_3^- + \text{SO}_4^{2-} + \text{SeO}_4^{2-}$ incubations were able to trap 17 ($\pm 1\%$)% and 6 ($\pm 0.4\%$)% of Se in the biofilm matrix with only 59 ($\pm 1\%$)% and 48 ($\pm 5\%$)% being released in the effluent, respectively (Table S1); a Se effluent mass balance is presented in Fig. 4. Results indicated that total Se detected in the effluent samples was mainly due to incomplete reduction of Se oxyanions (SeO_4^{2-} and SeO_3^{2-}). It should be considered that the biomass samples were randomly selected and biofilm heterogeneity might introduce some discrepancy in closing the overall Se mass balance. In addition, effluent sampling was conducted only once a day and considered representative; possible fluctuations in the effluent concentrations within the day might have occurred. Therefore, discrepancies in the Se mass balance are likely due to small sample sizes and random selection.

EDX results are shown in Fig. S4(a) while SEM images of biofilms grown under different growth conditions are shown in Fig. S4(b) to S4(e). Apart from carbon and oxygen signals emanating from the organic biofilm matrix, no other elements were present in detectable quantities for biofilms developed in the absence of

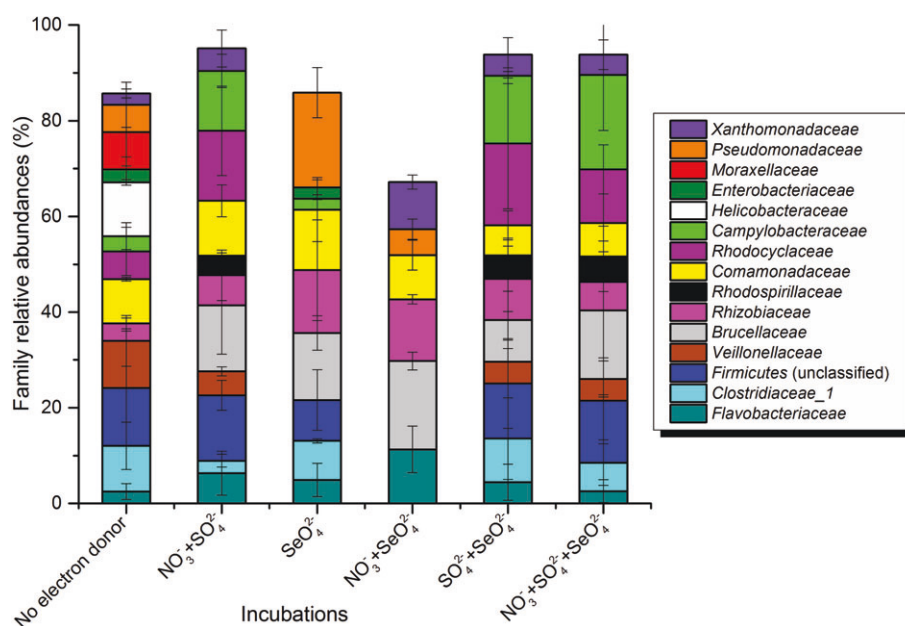


Figure 3. Relative abundances of microbial groups (as family phylotypes) in biofilm samples of each incubation. Relative abundances <1% are not displayed.

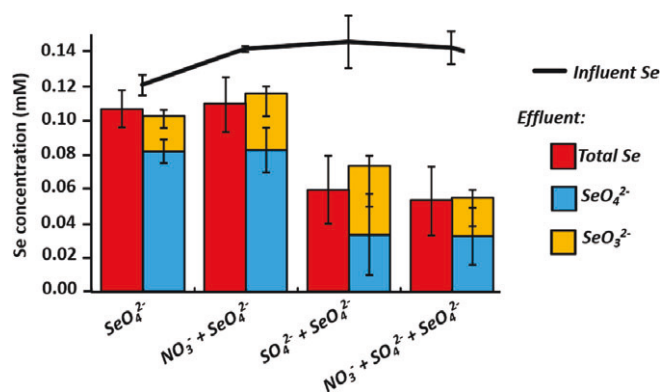


Figure 4. Effluent Se mass balance averaged over 10 days of continuous biofilm growth in DFRs fed with Se-contaminated wastewater and different co-electron acceptors.

external electron acceptors (Fig. S5). Biofilms formed in the presence of SeO_4^{2-} contained spherical nanoparticles and the spheres were identified to contain Se (Fig. S4). Biofilms incubated with SeO_4^{2-} alone, $\text{NO}_3^- + \text{SeO}_4^{2-}$ and $\text{NO}_3^- + \text{SO}_4^{2-} + \text{SeO}_4^{2-}$ showed similar EDX spectra, composed of mainly carbon and oxygen peaks with a significant Se signal. EDX spectra of $\text{SO}_4^{2-} + \text{SeO}_4^{2-}$ incubations indicated the presence of both Se and S in the ratio of approximately 3.5:1.

DISCUSSION

Influence of co-electron acceptors on Se removal and microbial community structure

Effect of SO_4^{2-}

Removal of Se was greatly influenced by the presence of SO_4^{2-} (Table 1) showing significantly higher removal efficiencies for both total Se and SeO_4^{2-} compared with SO_4^{2-} -free treatments. Promotion of Se removal in the presence of SO_4^{2-} could be due to the microbial community developed under different

incubation conditions (Fig. 3), leading to different biomass accumulation (Table 2), or increased biofilm activity (assessed via lactate consumption, Table 1).

In biofilms grown only with SeO_4^{2-} , a large percentage of the community consisted of *Pseudomonadaceae*. A number of *Pseudomonas* spp. are known to be capable of both SeO_4^{2-} and SeO_3^{2-} reduction to Se^0 .²⁷ A low relative abundance of *Pseudomonas* spp. was detected in biofilms formed in the other incubations, particularly those grown with SO_4^{2-} . This might indicate the development of a microbial community well-adapted to the reduction of SeO_4^{2-} in the biofilms grown only with SeO_4^{2-} . Biofilm communities grown in the presence of SO_4^{2-} ($\text{NO}_3^- + \text{SO}_4^{2-}$, $\text{SO}_4^{2-} + \text{SeO}_4^{2-}$ and $\text{NO}_3^- + \text{SO}_4^{2-} + \text{SeO}_4^{2-}$) contained an abundance of both known sulfate reducing bacteria (SRB, e.g. *Firmicutes*) and denitrifying bacteria (e.g. *Campylobacteraceae*, *Brucellaceae* and *Rhodocyclaceae*). *Sulfurospirillum* spp. represented about 88% of the *Campylobacteraceae* and have been described as SeO_4^{2-} respiring bacteria. *Sulfurospirillum* spp. are also able to grow under microaerobic conditions and most species can respire NO_3^- .^{6,10} Similarly, various members of the *Rhodocyclaceae* (i.e. *Zoogloea* sp. and *Azospira* sp.) can utilize both NO_3^- and SeO_3^{2-} as electron acceptor and have been found in biofilms growing in Se-containing medium.^{28,29} A number of unclassified members of the *Firmicutes* (containing the second largest known group of SRB, i.e. *Desulfovibrio*) were also detected in the presence of SO_4^{2-} (Fig. 3).

SeO_4^{2-} removal does not necessarily require Se-specific bacteria such as Se-respiring bacterial strains that can use SeO_4^{2-} as terminal electron donor to support growth. SeO_4^{2-} can be reduced to Se^0 through nonspecific mechanisms in the presence of SRB and denitrifying bacteria using assimilatory or dissimilatory pathways.³⁰ However, for some microorganisms (e.g. *Thauera selenatis* and *Sulfospirillum barnesii*) dissimilatory reduction of SeO_4^{2-} can support growth via anaerobic respiration, while in other cases (e.g. SRB) reduction of Se oxyanions can be part of a detoxification response or may be an adventitious reaction catalyzed by enzymes with a principally different function.^{30,31} This is evident in the SeO_4^{2-} only biofilm where, although a Se-reducing

community developed, biomass accumulation and lactate consumption was poor, possibility leading to poor Se removal. In contrast, biofilms grown with SO_4^{2-} showed substantially higher biomass accumulation and lactate consumption compared with incubations without SO_4^{2-} and could indicate that biofilms grown with SO_4^{2-} were more metabolically active. It is possible that sulfide precipitates contributed to the higher dry weight biomass of the incubations with SO_4^{2-} . However, it should be noted that in the SO_4^{2-} incubation with SeO_4^{2-} , only 4 mmol day^{-1} SO_4^{2-} was removed from the supplied 44 mmol day^{-1} . In addition, even with the increase in SO_4^{2-} removal rate in the $\text{NO}_3^- + \text{SO}_4^{2-}$ incubations of 7 mmol day^{-1} , the dry weight biomass was the same as those of the $\text{SO}_4^{2-} + \text{SeO}_4^{2-}$ and the $\text{NO}_3^- + \text{SO}_4^{2-} + \text{SeO}_4^{2-}$ incubations. Therefore, the contribution of sulfide deposits to the increase to biomass dry weight was likely negligible.

Tomei *et al.*³² reported similar results when studying the effects of SO_4^{2-} and SeO_4^{2-} on a pure culture of *Desulfovibrio desulfuricans*; higher biomass accumulation was observed when *D. desulfuricans* was grown in the presence of both SO_4^{2-} and SeO_4^{2-} , while lower biomass accumulation was observed when the *D. desulfuricans* biofilm was grown without SO_4^{2-} and only in the presence of SeO_4^{2-} . Lower cell growth of SRB cells due to SeO_4^{2-} can be attributed to SeO_4^{2-} interference with SO_4^{2-} activation and SeO_4^{2-} metabolism in SRB cells. The authors postulated that the inhibition of *D. desulfuricans* growth in the absence of SO_4^{2-} is due to the structural similarity between the Se and S atoms. Se oxyanions can act as S analogues, stopping SO_4^{2-} activation and disrupting both assimilatory and dissimilatory SO_4^{2-} reducing pathways,^{12,33} thereby reducing SRB cell growth.^{32,34}

Another reason for the increase in Se removal in the presence of SO_4^{2-} could be related to abiotic reactions possibly occurring between Se oxyanions and S compounds within the biofilm matrix. In the experiment by Hockin and Gadd⁴ using *Desulfomicrobium norvegicum* biofilms grown at 30°C and pH 7.0, formation of Se^0 was noted as a result of abiotic reduction of SeO_3^{2-} ($200 \mu\text{mol L}^{-1}$) by biogenic sulfide (10 mmol L^{-1}). The reduction of SeO_3^{2-} , the intermediate product between SeO_4^{2-} and Se^0 , by biogenic sulfide could have contributed to the more complete removal of SeO_4^{2-} . In the work presented here, there was no measurable dissolved sulfide in the effluent detected for any of the incubations (detection limit approximately 0.1 mmol L^{-1}). This could indicate either usage of sulfide for abiotic reduction or sulfur entrapment within the biofilm. Though it is difficult to properly quantify the abiotic reactions that were occurring within the biofilm, it is possible that interactions between SeO_3^{2-} and biogenic sulfide occurred when the biofilms were grown in the presence of $\text{SO}_4^{2-} + \text{SeO}_4^{2-}$.

Effect of NO_3^-

In contrast to SO_4^{2-} , NO_3^- did not have a stimulating effect on the removal of Se in the biofilm systems showing a similar Se removal efficiency, biomass accumulation and lactate consumption to biofilms grown in the presence of solely SeO_4^{2-} . In addition, NO_3^- removal was poor in the incubations void of SO_4^{2-} . SO_4^{2-} does not typically have a negative effect on NO_3^- reduction, considering the highly thermodynamically favorable denitrification reactions compared with reduction of the other oxyanions investigated. In most biological wastewater treatment studies, the presence of other oxyanions has not been identified as a detrimental factor for NO_3^- removal.^{10,11,14,35}

Microbial communities in biofilms grown in the presence of $\text{NO}_3^- + \text{SeO}_4^{2-}$ showed three dominant bacterial families: *Comamonadaceae*, *Rhizobiaceae* and *Brucellaceae*, all known for their

denitrifying bacterial members, which are often found in freshwater or soil and can play an important role in the nitrogen cycle. In addition, although *Pseudomonadaceae* are also known for their NO_3^- respiring bacterial members, there was only a small relative abundance percentage found in biofilms grown under $\text{NO}_3^- + \text{SeO}_4^{2-}$ conditions ($5.4 \pm 2.1\%$ RA) compared with biofilms grown with SeO_4^{2-} alone ($19.8 \pm 2.1\%$ RA). Some members of the *Comamonadaceae* (e.g. *Comamonas* sp.) are described to be SeO_3^{2-} reducers,²⁹ while *Ochrobactrum* spp. is capable of reducing SeO_3^{2-} and tellurite to Se^0 and Te^0 nanoparticles, respectively.³⁶ However, there is little information available on the potential role of these organisms in the reduction of SeO_4^{2-} . On the other hand, *Rhizobium* spp. (constituting $\sim 79\%$ of the *Rhizobiaceae*) have been studied by Hunter and Manter³⁷ under denitrifying conditions and it was observed that under anoxic conditions, *Rhizobium* sp. growth was dependent on the presence of NO_3^- and that NO_3^- was necessary to facilitate SeO_4^{2-} or SeO_3^{2-} reduction.

While the microbial community analyses showed the presence of denitrifiers (Fig. 3), the low NO_3^- and SeO_4^{2-} removal efficiencies (Table 1) could possibly be due to an overall decrease in microbial activity in the absence of SO_4^{2-} , which is supported by the low lactate consumption (average removal efficiency $48 \pm 9\%$) and low biomass production (averaged $2.9 \pm 1 \text{ mg TS cm}^{-2}$) in the SeO_4^{2-} and $\text{NO}_3^- + \text{SeO}_4^{2-}$ incubations. Another explanation for the low NO_3^- and SeO_4^{2-} removal could be that the inoculum used for the study, identified to be dominated by methanogens and SRB,¹⁶ contained a low denitrifying population at the initial stage of incubation. Though microbial communities were characterized, this was conducted at the end of a 12-day experimental run (2 days of batch incubation and 10 days of continuous operation) and a denitrifying population might not have developed well during these relatively short-term experiments. This could indicate that the inoculum was indeed predisposed to SO_4^{2-} reducing conditions and would have required more time to establish a denitrifying microbial community. Hence, longer term monitoring of the microbial community, the evaluation of different inocula and their ability to adapt to the treatment conditions should be considered in future studies.

Alternatively, competition for reductases and/or intermediates of SeO_4^{2-} reduction might have occurred. In the case of SRBs, Hockin and Gadd,¹² who also observed increased Se removal efficiencies in the presence of high SO_4^{2-} concentrations (28 mmol L^{-1}), proposed that SeO_4^{2-} reduction takes place in the periplasm of SRBs, allowing for simultaneous reduction without competition between SeO_4^{2-} and SO_4^{2-} . For certain denitrifying or Se-reducing bacteria (i.e. *Enterobacter cloacae*), membrane-bound NO_3^- reductases (*Nar*), periplasmic NO_3^- reductases (*Nap*) and SeO_4^{2-} reductases (*Ser*) have all been shown to catalyze the reduction of SeO_4^{2-} to SeO_3^{2-} .³⁸ Furthermore, some denitrifiers (i.e. *Rhizobium sllae* and *Sulfurospirillum barnesii*) are only capable of reducing SeO_4^{2-} to SeO_3^{2-} and require another intermediate, such as nitrite, to further reduce SeO_3^{2-} to Se^0 via nitrite reductases, while others can only reduce either SeO_4^{2-} to SeO_3^{2-} or SeO_3^{2-} to Se^0 .^{10,39} As such, it is possible that low SeO_4^{2-} removal under $\text{NO}_3^- + \text{SeO}_4^{2-}$ incubation could be due to the lack of accumulated intermediate, i.e. nitrite, or specific organisms to properly facilitate the full reduction process from SeO_4^{2-} to Se^0 .

Se immobilization and biofilm response to Se exposure

The biofilms in the DFR appeared to be the thinnest when only SeO_4^{2-} was fed into the system, while those grown with SeO_4^{2-} plus co-electron acceptors were generally thicker (Fig. 2). Thinner

biofilms could be a result of stress from or toxicity of SeO_4^{2-} to the biomass, e.g. production of intermediate SeO_3^{2-} or entrapment of biogenic Se^0 . Densification of fungal biofilms upon exposure to SeO_3^{2-} has been described for *Phanerochaete chrysosporium* pellets.⁴⁰ The authors attributed this densification to a stress response due to the presence of SeO_3^{2-} as well as the deposition of biogenic Se^0 within the pellets. Biogenic Se^0 nanoparticles have been described to harbor antimicrobial and antibiofilm activities due to the production of reactive oxygen species.³⁶ However, this study did not monitor whether the dense biofilms indeed produced reactive oxygen species.

One of the main issues in biological treatment of Se-laden wastewaters is the release of colloidal Se^0 into the aqueous phase, which not only potentially compromises discharge criteria but also raises questions regarding the fate and stability of Se^0 in the environment.⁴¹ Additional chemical post-treatment methods such as electrocoagulation and precipitation might be required to ensure the removal of Se^0 colloidal particles.^{9,42} Therefore, this study investigated SeO_4^{2-} transformation, retention and immobilization of biogenic Se^0 in the biofilms.

This study provides strong evidence of Se immobilization within the biofilm matrix: (1) visual red deposits inside the biofilms (Fig. 1); (2) detection of Se within the biofilm matrix; and (3) Se-containing spherical particles in the biofilms revealed by SEM–EDX analysis (Fig. S4). Biofilm images revealed an orange-red coloration of biofilms (Fig. 1), particular those grown in the presence of SO_4^{2-} , which is a strong indication of a transformation of SeO_4^{2-} to biogenic Se^0 and its retention within the biofilm.⁴³ In addition, effluent Se mass balance calculations showed a negligible release of colloidal Se^0 (estimated as the difference between total Se and Se oxyanion concentration) in the effluent of the biofilm reactors (Fig. 4). HPLC-ICP-MS analyses of effluent samples revealed no peaks for other dissolved Se compounds aside from SeO_3^{2-} and SeO_4^{2-} (data not shown). Visually, no reddish color (indication of colloidal Se^0) was observed in the effluent for any of the incubations. Instead, incubations with SO_4^{2-} showed a yellowish coloration in the effluent, while the effluents of treatments without SO_4^{2-} remained mostly clear to slightly whitish (Fig. S6(a)). Yellowish coloration could be an indication of elemental sulfur (S^0). This was confirmed by EDX analysis of dried effluent samples. The EDX spectra revealed S-associated peaks from effluent samples with yellowish color (Fig. S6(c)), while no S signal was detected in the clear-to-whitish effluent samples from incubations without SO_4^{2-} (Fig. S6(b)). Possible formation of Se-S particles inside the biofilms was indicated by the EDX spectra (Fig. S4(a)). Detection of Se-S particles were similarly observed by Davis *et al.*⁴⁴ during *in situ* SeO_4^{2-} bioprecipitation in a SO_4^{2-} reducing groundwater zone and by Hockin and Gadd⁴ under SO_4^{2-} reducing conditions in batch experiments investigating SeO_3^{2-} reduction.

This study indicates that the biofilms formed in the DFR retained Se^0 formed by microbial reduction within the biofilm matrix. In particular, biofilms formed in the presence of $\text{SO}_4^{2-} + \text{SeO}_4^{2-}$ accumulated more total Se in the biofilm matrix while exhibiting greater biomass growth and better SeO_4^{2-} removal. Treatment of Se-laden wastewaters coupled with SO_4^{2-} removal could have potential applications in the reuse of Se^0 through biological reduction of Se-oxyanions.^{9,20} However, Se recovery and purification techniques from biological systems are still largely unexplored and will require further research before actual large-scale application. However, this study did not evaluate the effect of other heavy metals, which might be present in mining wastewaters; this should be the focus of future studies.

Alternative nondestructive biofilm imaging techniques such as cryo-slicing coupled with low-temperature FESEM⁴ or synchrotron techniques such as X-ray fluorescence imaging and scanning transmission X-ray microscopy^{39,45} could be used in the future for investigation of the localization of the precipitated Se and S granules. This would allow further insights into the fate and behavior of Se within the biofilms as influenced by the presence of NO_3^- and/or SO_4^{2-} .

CONCLUSIONS

Effective SeO_4^{2-} removal through microbial reduction to elemental Se^0 and retention of biogenic elemental Se^0 within the biofilm matrix was demonstrated in drip flow biofilm reactors over a 10-day period. The experimental work conducted in this study has practical implications in industrial system management and the treatment of Se-laden wastewater containing high amounts of co-electron acceptors, i.e. NO_3^- and SO_4^{2-} . This study demonstrates that biofilms can be established in simulated mining wastewater and that SeO_4^{2-} removal efficiency by lactate-fed anaerobic biofilms can be affected by the presence of specific oxyanions. The presence of SO_4^{2-} in the synthetic wastewater significantly improved biofilm growth and the SeO_4^{2-} removal efficiency, whereas the presence of NO_3^- did not have a significant effect on SeO_4^{2-} removal by the biofilms. Thus, the presence of co-electron acceptors in Se-laden wastewater – and possibly even their addition – should be carefully considered, as it can be beneficial for Se removal. Electron acceptors also affected the morphology of the biofilms. Relatively thin biofilms were formed in the presence of SeO_4^{2-} alone, while thicker biofilms accumulated in the presence of NO_3^- or SO_4^{2-} , which could have implications for the management of biofilms in scaled-up operations. In addition, biogenic Se^0 was mainly retained within the biofilm matrix, which minimized the discharge of colloidal Se^0 in the treated water leaving the reactor. This indicates, overall, that anaerobic treatment using biofilm systems can be directly applied and is suitable for treating Se-laden wastewater with co-electron acceptors.

ACKNOWLEDGEMENTS

The authors would like to thank the following researchers from the Center for Biofilm Engineering at Montana State University for their help with various analyses: Dr Chiachi Hwang for carrying out cleanup and Illumina MiSeq analysis of biomass samples; Prof Ellen Lauchnor and Laura Dobeck for total selenium and selenium speciation analysis; Betsey Pitts for assistance in acquiring CLSM and other microscopy images; and Neerja Zambare for conducting SEM–EDX imaging analysis of biomass samples.

CONFLICT OF INTEREST

The authors declare no conflict of interest.

Supporting Information

Supporting information may be found in the online version of this article.

REFERENCES

- 1 Lenz M and Lens PNL, The essential toxin: the changing perception of selenium in environmental sciences. *Sci Total Environ* 407:3620–3633 (2009).

- 2 Wen H and Carignan J, Reviews on atmospheric selenium: emissions, speciation and fate. *Atmos Environ* **41**:7151–7165 (2007).
- 3 Tan LC, Nancharaiah YV, van Hullebusch ED and Lens PNL, Selenium: environmental significance, pollution, and biological treatment technologies. *Biotechnol Adv* **34**:886–907 (2016).
- 4 Hockin SL and Gadd GM, Linked redox precipitation of sulfur and selenium under anaerobic conditions by sulfate-reducing bacterial biofilms. *Appl Environ Microbiol* **69**:7063–7072 (2003).
- 5 Lemly AD, Teratogenic effects and monetary cost of selenium poisoning of fish in Lake Sutton, North Carolina. *Ecotoxicol Environ Saf* **104**:160–167 (2014).
- 6 Nancharaiah YV and Lens PNL, Ecology and biotechnology of selenium-respiring bacteria. *Microbiol Mol Biol Rev* **79**:61–80 (2015).
- 7 Mal J, Veneman WJ, Nancharaiah YV, van Hullebusch ED, Peijnenburg WJGM, Vijver MG and Lens PNL, A comparison of fate and toxicity of selenite, biogenically, and chemically synthesized selenium nanoparticles to zebrafish (*Danio rerio*) embryogenesis. *Nanotoxicology* **11**:87–97 (2017).
- 8 Nguyen VK, Park Y, Yu J and Lee T, Microbial selenite reduction with organic carbon and electrode as sole electron donor by a bacterium isolated from domestic wastewater. *Bioresource Technol* **212**:182–189 (2016).
- 9 Nancharaiah YV and Lens PNL, Selenium biomineralization for biotechnological applications. *Trends Biotechnol* **33**:1–8 (2015).
- 10 Oremland RS, Blum JS, Bindi AB, Dowdle PR, Herbel M and Stolz JF, Simultaneous reduction of nitrate and selenate by cell suspensions of selenium-respiring bacteria. *Appl Environ Microbiol* **65**:4385–4392 (1999).
- 11 Lai C-Y, Yang X, Tang Y, Rittmann BE and Zhao H-P, Nitrate shaped the selenate-reducing microbial community in a hydrogen-based biofilm reactor. *Environ Sci Technol* **48**:3395–3402 (2014).
- 12 Hockin S and Gadd GM, Removal of selenate from sulfate-containing media by sulfate-reducing bacterial biofilms. *Environ Microbiol* **8**:816–826 (2006).
- 13 Ontiveros-Valencia A, Penton CR, Krajmalnik-Brown R and Rittmann BE, Hydrogen-fed biofilm reactors reducing selenate and sulfate: community structure and capture of elemental selenium within the biofilm. *Biotechnol Bioeng* **113**:1736–1744 (2016).
- 14 Tan LC, Nancharaiah YV, van Hullebusch ED and Lens PNL, Effect of elevated nitrate and sulfate concentrations on selenate removal by mesophilic anaerobic granular sludge bed reactors. *Environ Sci: Water Res Technol* **4**:303–314 (2018).
- 15 van Ginkel SW, Yang Z, Kim B, Sholin M and Rittmann BE, The removal of selenate to low ppb levels from flue gas desulfurization brine using the H₂-based membrane biofilm reactor (MBfR). *Bioresource Technol* **102**:6360–6364 (2011).
- 16 Roest K, Heilig HGH, Smidt H, De Vos WM, Stams AJM and Akkermans ADL, Community analysis of a full-scale anaerobic bioreactor treating paper mill wastewater. *Syst Appl Microbiol* **28**:175–185 (2005).
- 17 Stams AJM, Grolle KCF, Frijters CTM and van Lier JB, Enrichment of thermophilic propionate-oxidizing bacteria in syntrophy with *Methanobacterium thermoautotrophicum* or *Methanobacterium thermoformicum*. *Appl Environ Microbiol* **58**:346–352 (1992).
- 18 Stover EL, Pudvay M, Kelly RF and Lau AO, Biological treatment of flue gas desulfurization wastewater. Proceeding Engineer's Society of Western Pennsylvania, IWC-07-49 (2006).
- 19 Goeres DM, Hamilton MA, Beck NA, Buckingham-Meyer K, Hilyard JD, Loetterle LR *et al.*, A method for growing a biofilm under low shear at the air-liquid interface using the drip flow biofilm reactor. *Nat Protoc* **4**:783–788 (2009).
- 20 Jain R, Seder-Colomina M, Jordan N, Dessi P, Cosmidis J, van Hullebusch ED *et al.*, Entrapped elemental selenium nanoparticles affect physicochemical properties of selenium fed activated sludge. *J Hazard Mater* **295**:193–200 (2015).
- 21 Manteca Á, Fernández M and Sánchez J, A death round affecting a young compartmentalized mycelium precedes aerial mycelium dismantling in confluent surface cultures of *Streptomyces antibioticus*. *Microbiology* **151**:3689–3697 (2005).
- 22 Lueders T, Manefield M and Friedrich MW, Enhanced sensitivity of DNA- and rRNA-based stable isotope probing by fractionation and quantitative analysis of isopycnic centrifugation gradients. *Environ Microbiol* **6**:73–78 (2004).
- 23 Takahashi S, Tomita J, Nishioka K, Hisada T and Nishijima M, Development of a prokaryotic universal primer for simultaneous analysis of Bacteria and Archaea using next-generation sequencing. *PLOS One* **9**:e105592 (2014).
- 24 Schloss PD, Westcott SL, Ryabin T, Hall JR, Hartmann M, Hollister EB *et al.*, Introducing mothur: open-source, platform-independent, community-supported software for describing and comparing microbial communities. *Appl Environ Microbiol* **75**:7537–7541 (2009).
- 25 Li D-B, Cheng Y-Y, Wu C, Li W-W, Li N, Yang Z-C *et al.*, Selenite reduction by *Shewanella oneidensis* MR-1 is mediated by fumarate reductase in periplasm. *Sci Rep* **4**:3735 (2014).
- 26 Cord-Ruwisch R, A quick method for the determination of dissolved and precipitated sulfides in cultures of sulfate-reducing bacteria. *J Microbiol Methods* **4**:33–36 (1985).
- 27 Gonzalez-Gil G, Lens PNL and Saikaly PE, Selenite reduction by anaerobic microbial aggregates: microbial community structure, and proteins associated to the produced selenium spheres. *Front Microbiol* **7**:571 (2016).
- 28 Hunter WJ, An *Azospira oryzae* (*syn* *Dechlorosoma suillum*) strain that reduces selenate and selenite to elemental red selenium *Curr Microbiol* **54**:376–381 (2007).
- 29 Fakra SC, Luef B, Castelle CJ, Mullin SW, Williams KH, Marcus MA *et al.*, Correlative cryogenic spectro-microscopy to investigate Selenium bioreduction products. *Environ Sci Technol* <https://doi.org/10.1021/acs.est.5b01409> (2015).
- 30 Eswayah AS, Smith TJ and Gardiner PHE, Microbial transformations of selenium species of relevance to bioremediation. *Appl Environ Microbiol* **82**:4848–4859 (2016).
- 31 Muyzer G and Stams AJM, The ecology and biotechnology of sulphate-reducing bacteria. *Nat Rev Microbiol* **6**:441–454 (2008).
- 32 Tomei FA, Barton LL, Lemanski CL, Zocco TG, Fink NH and Sillerud LO, Transformation of selenate and selenite to elemental selenium by *Desulfovibrio desulfuricans*. *J Ind Microbiol* **14**:329–336 (1995).
- 33 Bulska E, Wysocka IA, Wierzbicka MH, Proost K, Janssens K and Falkenberg G, *In vivo* investigation of the distribution and the local speciation of selenium in *Allium cepa* L. by means of microscopic x-ray absorption near-edge structure spectroscopy and confocal microscopic x-ray fluorescence analysis. *Anal Chem* **78**:7616–7624 (2006).
- 34 Malagoli M, Schiavon M, dall'Acqua S and Pilon-Smits EAH, Effects of selenium biofortification on crop nutritional quality. *Front Plant Sci* **6**:1–5 (2015).
- 35 Lenz M, Enright AM, O'Flaherty V, van Aelst AC and Lens PNL, Bioaugmentation of UASB reactors with immobilized *Sulfurospirillum barnesii* for simultaneous selenate and nitrate removal. *Appl Microbiol Biotechnol* **83**:377–388 (2009).
- 36 Zonaro E, Lampis S, Turner RJ, Junaid S and Vallini G, Biogenic selenium and tellurium nanoparticles synthesized by environmental microbial isolates efficaciously inhibit bacterial planktonic cultures and biofilms. *Front Microbiol* **6**:658 (2015).
- 37 Hunter WJ and Manter DK, Reduction of selenite to elemental red selenium by *Rhizobium* sp. strain B1. *Curr Microbiol* **55**:344–349 (2007).
- 38 Ridley H, Watts CA, Richardson DJ and Butler CS, Resolution of distinct membrane-bound enzymes from *Enterobacter cloacae* SLD1a-1 that are responsible for selective reduction of nitrate and selenate oxyanions. *Appl Environ Microbiol* **72**:5173–5180 (2006).
- 39 Yang SI, Lawrence JR, Swerhone GDW and Pickering IJ, Biotransformation of selenium and arsenic in multi-species biofilm. *Environ Chem* **8**:543–551 (2011).
- 40 Espinosa-Ortiz EJ, Pechaud Y, Lauchnor E, Rene ER, Gerlach R, Peyton BM *et al.*, Effect of selenite on the morphology and respiratory activity of *Phanerochaete chrysosporium* biofilms. *Bioresource Technol* **210**:138–145 (2016).
- 41 Buchs B, Evangelou MWH, Winkel LHE and Lenz M, Colloidal properties of nanoparticulate biogenic selenium govern environmental fate and bioremediation effectiveness. *Environ Sci Technol* **47**:2401–2407 (2013).
- 42 Staicu LC, van Hullebusch ED and Lens PNL, Production, recovery and reuse of biogenic elemental selenium. *Environ Chem Lett* **13**:89–96 (2015).

- 43 Dessi P, Jain R, Singh S, Seder-Colomina M, van Hullebusch ED, Rene ER *et al.*, Effect of temperature on selenium removal from wastewater by UASB reactors. *Water Res* **94**:146–154 (2016).
- 44 Davis AC, Patterson BM, Grassi ME, Robertson BS, Prommer H and McKinley AJ, Effects of increasing acidity on metal(loid) bioprecipitation in groundwater: column studies. *Environ Sci Technol* **41**:7131–7137 (2007).
- 45 Yang SI, George GN, Lawrence JR, Kaminskyj SGW, Dynes JJ, Lai B *et al.*, Multispecies biofilms transform selenium oxyanions into elemental selenium particles: Studies using combined synchrotron x-ray fluorescence imaging and scanning transmission x-ray microscopy. *Environ Sci Technol* **50**:10343–10350 (2016).